Nanosecond time-resolved XFEL structure analyses of bovine cytochrome c oxidase reveals the timing of proton-pump channel closure

Mitochondria occupy a substantial portion of the cytoplasmic volume of animal cells, and produce ATP used in a wide range of cellular processes. The mitochondrial ATPase synthesizes ATP using a transmembrane proton motive force, which is generated by respiratory enzymes. Cytochrome c oxidase (CcO), the terminal enzyme of cellular respiration, reduces O_2 to H_2O; this reaction is coupled to proton pumping across the mitochondrial inner membrane (Fig. 1(a)). Bovine CcO is a large transmembrane protein that exists as a 420-kDa dimer in the crystalline state. Each monomer includes four redox active metal sites (Fe_a, Fe_{a3}, Cu_B, and Cu_A). The O_2 reduction site contains Cu_B and Fe_{a3} (Fig. 1(b)). O_2 is transiently trapped at Cu_B before binding to Fe_{a3} [1-2]. Via Fe_a, four electrons are sequentially transferred from cytochrome c at the P-side to O_2 at Fe_{a3} (but not to O_2 at Cu_B), while four protons are actively transferred from the N-side (the P- and N-sides designate the outside and inside of the mitochondrial inner membrane, which are positively and negatively charged, respectively). The protons are transferred through the H-pathway, which consists of a water channel (light-blue arrows in Fig. 1) and a hydrogen bond network (red arrows in Fig. 1) operating in tandem. The water channel in the H-pathway includes water cavities.

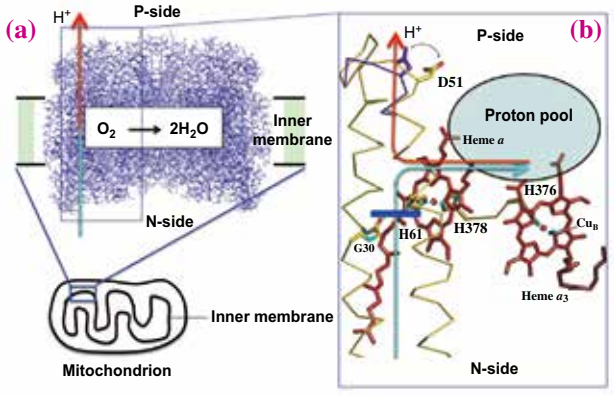

Fig. 1. Cytochrome c oxidase in the mitochondrial inner membrane. (Bottom **a**) Schematic drawing of a mitochondrion. (Top **a**) Structure of bovine CcO with dimeric structure. The enzyme reduces O_2 to H_2O using electrons from cytochrome c and pumps protons through the H-pathway (indicated by a light blue line and a red arrow from the N-side to P-side). (**b**) A close-up view of the H-pathway, proton pool, heme a, and O_2 reduction site consisting of heme a_3 and Cu_B. The H-pathway consists of a water channel (light-blue arrow) and a hydrogen bond network (red arrow). The blue line in the water channel is a gate operated by a conformational change in helix X. When the gate is opened, four protons accumulate in the proton pool. Pumping of each proton to the P-side is coupled with transfer of an electron from cytochrome c to heme a_3 via heme a.

The proton-pumping step is divided into two stages. First, four protons accumulate in the proton pool through the water channel of the H-pathway. As each electron is transferred from heme a to heme a_3, a proton is transferred from the proton pool to the P-side through the hydrogen bond network of the H-pathway, driven by electrostatic repulsion between the proton and the net positive charge of Fe_a. The water channel must be closed during electron transfer from heme a to heme a_3; if it were to remain open, spontaneous backflow of the collected protons would occur. To elucidate the channel closure mechanism, the opening of the channel, which occurs upon release of CO from CcO, has been investigated by newly developed time-resolved X-ray free-electron laser and infrared techniques with nanosecond time resolution [3]. CO has been widely used to probe the active sites of heme proteins.

In this project, we used a newly developed serial femtosecond rotational crystallography (SF-ROX) method [4] based on analysis of many large single crystals. Furthermore, we used time-resolved IR to monitor CO movements in CcO crystals.

Time-resolved infrared spectral changes occurring during CO migration in the single crystalline state of CcO were traced at 4°C from 20 ns to 500 ms after flash photolysis of the fully reduced CO-bound state. The spectral changes suggested that 100% of CO molecules moved from the Fe_{a3} site to the Cu_B site at 20 ns; about 76% of CO disappeared from the O_2 reduction center, and about 24% of CO remained at Cu_B at 100 μs, and 100% of CO returned to the Fe_{a3} site at 100 μs after photolysis.

The XFEL diffraction data obtained without pump laser irradiation (dark) and at 20 ns and 100 μs after pump laser irradiation were collected from 40, 24, and 43 crystals, respectively, all at 4°C. The experimental setup at SACLA EH4c/**BL3** was as described for a previous XFEL experiment for damage-free crystallography [4]. The structures of three states were determined: at 2.2 Å resolution for the dark and 100-μs crystals, and at 2.4 Å resolution for the 20-ns crystal. Refinements converged well to R_{work} = 0.173, 0.185, and 0.173, and R_{free} = 0.202, 0.229, and 0.208, for dark, 20-ns, and 100-μs crystals, respectively.

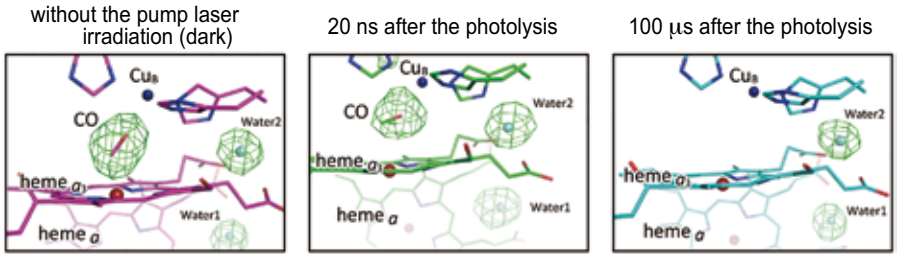

Fig. 2. Structures of the O_2 reduction sites of the CO-bound fully reduced state of the dark, 20-ns, and 100-μs structures. F_o-F_c difference electron density maps at 3.5σ and structural models. Purple spheres indicate iron ions, blue spheres copper ions, and light blue spheres the oxygen atoms of water molecules. Blue and red sticks indicate nitrogen and oxygen atoms, respectively. Purple, green, and light blue sticks indicate other atoms of dark, 20-ns, and 100-μs structures, respectively. CO, water 1, and water 2 were not included in the structural refinement. No significant electron density assignable to the CO molecule between Fe_{a3} and Cu_B is detectable in the 100-μs structure at the σ level depicted in the figure.

The CO molecules in the three states were located in the F_o-F_c difference maps (Fig. 2), and the structural changes of helix X are shown in the F_o-F_c difference map for two types of models (Fig. 3). These structural analyses indicated that the CO molecule moved from the Fe_{a3} site to the Cu_B site 20 ns after photolysis and disappeared from the O_2 reduction center 100 μs after photolysis. Moreover, the structures of helix X in the dark and 20-ns crystals were in a closed form that blocked proton transfer, whereas in the 100-μs crystal, helix X changed to an open conformation at a rate of 45% that opened a proton transfer gate of the water channel in the H-pathway. Thus, CO release from Cu_B to the outside of the O_2 reduction center drives the transition of the closed structure to the open structure.

Based on our inspection of structural features of hemes and helix X for all three states, we propose a mechanism for closure of the water channel. When the O_2 reduction site is in the fully reduced state, the water channel is opened, and protons are transferred from the N-side to the proton pool. Once O_2 is trapped at Cu_B, closure of the water channel is induced as follows: (i) The plane of Fe_{a3} migrates; (ii) van der Waals interactions are altered between the vinyl group of Fe_{a3} and L381 of the helix X; and (iii) a bulge forms at S382 when L381 moves to close the water channel. This process is followed by O_2 transfer to Fe_{a3} (1-2), yielding $Fe_{a3}{}^{3+}$-$O_2{}^{-}$, which readily extracts electrons from Fe_a when it is reduced. Oxidation of Fe_a induces electrostatic repulsion against protons in the storage site. The closure of the water channel after O_2 migration to Cu_B, before formation of the Fe_{a3}-O_2 bond, causes obligatory pumping of protons to the P-side because the water channel has been closed.

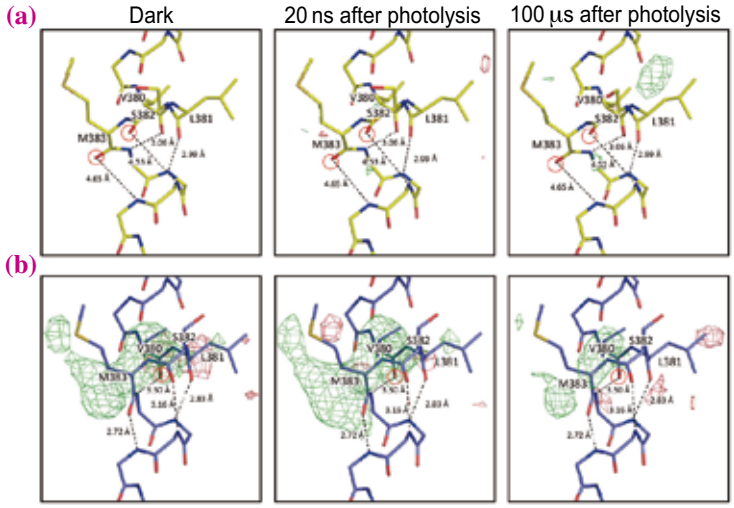

Fig. 3. F_o-F_c difference electron density maps of the dark, 20-ns, and 100-μs structures. The structural factors of Fc were calculated from the closed and open structures of helix X, with two bulges at S382 and M383 **(a)** and with one bulge at V380 **(b)**, and F_o-F_c difference electron density maps were drawn at 3.5σ along with the closed and open structures of helix X, respectively. Red circles mark the locations of the bulges.

Tomitake Tsukihara[a,b,*], Hideo Ago[c] and Shinya Yoshikawa[a]

[a] Graduate School of Life Science, University of Hyogo
[b] Institute for Protein Research, Osaka University
[c] RIKEN SPring-8 Center

*Email: tsuki@protein.osaka-u.ac.jp

References

[1] S. Yoshikawa *et al.*: Chem. Rev. **115** (2015) 1936.
[2] P.R. Rich and A. Maréchal: J. R. Soc. Interface **10** (2013) 20130183.
[3] *A. Shimada, M. Kubo, S. Baba, K. Yamashita, K. Hirata, G. Ueno, T. Nomura, T. Kimura, K. Shinzawa-Itoh, J. Baba, K. Hatano, Y. Eto, A. Miyamoto, H. Murakami, T. Kumasaka, S. Owada, K. Tono, M. Yabashi, Y. Yamaguchi, S. Yanagisawa, M. Sakaguchi T. Ogura, R. Komiya, J. Yan, E. Yamashita, M. Yamamoto, H. Ago, S. Yoshikawa, T. Tsukihara: Sci. Adv.* ***3*** *(2017) e1603042.*
[4] K. Hirata *et al.*: Nat. Methods **11** (2014) 734.